coatings

MDPI

Article

Low-Stress Abrasion of Novel Ni-P-Tribaloy Composite Coating

Ahmed Mabrouk [1,*], Zoheir Farhat [1,*] and Md. Aminul Islam [2]

[1] Department of Mechanical Engineering, Dalhousie University, 1360 Barrington Street, Halifax, NS B3J 2X4, Canada
[2] National Research Council Canada, 4250 Wesbrook Mall, Vancouver, BC V6T 1W5, Canada
* Correspondence: ahmed.mabrouk@dal.ca (A.M.); zoheir.farhat@dal.ca (Z.F.)

Abstract: Degradation of industrial machinery through wear can be mitigated with the deposition of protective coatings to reduce maintenance costs and prolong their service lifespans. Electroless nickel-based composite coatings is one possible method used to provide this protection. The addition of Tribaloy (CoMoCrSi alloy) particles has been found to produce composite coatings with high toughness. In this work, electroless Ni-P-Tribaloy composite coatings were plated on AISI 1018 steel substrates and subjected to low-stress abrasion tests following ASTM G65 standards to investigate the abrasion of the coating. The test was performed at 10 revolution increments, with a 45 N applied load, until coating failure was observed and the measured abrasion was reported as volume loss. The two Ni-P-Tribaloy coating samples lasted for 90 and 100 revolutions, exhibiting a wear rate of 0.170 mm^3 per revolution, compared to 0.135 mm^3 per revolution for the Ni-P coatings. The abrasive wear mechanism in the Ni-P-Tribaloy coating was found to be plowing of the matrix around the Tribaloy particles, followed by the removal of the particles once they are protruding, which subsequently contributes to the three-body wear of the coating. The particle removal was accelerated at the coating particle-matrix interface. It is concluded that the size of the Tribaloy is a major factor, and we recommend that further studies be carried out using finer particles to improve the wear resistance of the Ni-P-Tribaloy coating.

Keywords: electroless nickel; Ni-P-Tribaloy coating; abrasive wear; metal matrix composites (MMC); wear mechanisms; ASTM G65

Citation: Mabrouk, A.; Farhat, Z.; Islam, M.A. Low-Stress Abrasion of Novel Ni-P-Tribaloy Composite Coating. *Coatings* **2023**, *13*, 1647. https://doi.org/10.3390/coatings13091647

Academic Editor: Manuel António Peralta Evaristo

Received: 12 August 2023
Revised: 13 September 2023
Accepted: 18 September 2023
Published: 20 September 2023

1. Introduction

Wear plays a major role in the degradation of machinery across various industries. Most engineering failures initiate from the surface; therefore, the application of protective coatings is vital to prolong the components' lifespan and minimize the associated service and maintenance costs [1–3]. For many years, electroless nickel-phosphorus (Ni-P) coatings have been utilized as protective coatings in the oil and gas, aerospace, and automotive industries, among others, due to the technique's ease of application and the unique resulting properties of the coatings including high wear and corrosion resistance, hardness, lubricity, and adhesion [4,5]. Electroless nickel is a coating technique involving the chemical reduction of nickel in an aqueous solution driven by a reducing agent, typically sodium hypophosphite, supplying the driving force for this autocatalytic process [6,7]. Several Ni-P-based composite coatings have been developed through the co-deposition of second-phase particles, such as WC and SiO_2, within the metallic Ni-P matrix [8,9]. Developing composite coatings has been proven to alter selective properties of the Ni-P coating, based on the type of particles used. For example, soft particles like Polytetrafluoroethylene (PTFE) lower the coefficient of friction and provide good lubrication while sacrificing hardness, in contrast to hard particles like SiC, which provides the opposite for use in applications where high hardness is required [10–12].

The focus of this work is Ni-P-Tribaloy composite coatings which consist of an electroless Ni-P matrix with Tribaloy as second-phase reinforcement particles. Tribaloy alloys are

a series of Co-based alloys composed of CoMoCrSi. These alloys possess excellent wear and corrosion resistance as a result of their unique composition. The main alloying elements are Cr, Mo, and Si, with each element influencing the alloy's properties. The inclusion of Mo and Si is vital for wear resistance, and Cr enhances the corrosion resistance [13,14]. Tribaloys consist of Laves intermetallic phases dispersed in a solid solution of Co, and the fraction of the Laves phase is dictated by the composition of the alloy. Mo and Si are added in excess of their respective solubility limits to promote the precipitation of the Laves phase [15–17]. Tribaloy T-800 is one of the most common commercial compositions, consisting of 28.5 wt.% molybdenum, 17.5 wt.% chromium, 3.4 wt.% silicon, and balance cobalt. It exhibits the largest content of the Laves phase, imparting it with high wear resistance and hardness [18]. Previous work by the authors has established Tribaloy particles as a promising candidate to be deposited by electroless plating, creating Ni-P-Tribaloy composite coatings [19].

Abrasion is damage to a solid surface that is in sliding contact with a harder material. There are two forms of abrasive wear: two-body wear occurs when asperities on a harder or rougher surface slides against a softer surface, and three-body wear occurs when loose hard particles are trapped between two sliding surfaces [20,21]. Plowing and cutting are two of the main wear mechanisms that result from abrasive wear. Cutting refers to a harder asperity cutting the softer material forming a chip that is removed as wear debris. Plowing refers to the sideways displacement of the material from the surface forming a groove with a ridge on both sides [20,22]. In an ideal case, micro-plowing due to a single pass of one hard particle does not result in material removal from the surface; however, material loss will occur through multiple abrasive particles acting simultaneously [23]. Low-stress abrasion testing, using the ASTM G65 standard [24], is a dry sand/rubber wheel abrasion test that is often used to simulate wear in different applications [23–25]. In low-stress abrasion, there is low applied contact pressure between the test specimen and the abrasive particles, and the particles remain unbroken during the wear process, as opposed to high-stress abrasion, where they are crushed. Higher contact pressure is associated with deeper indentations and promotes the cutting mechanism [21,23]. The ASTM G65 test is a standardized abrasion test that allows for the comparison of materials based on their measured volume loss following this test procedure. This test is essential when investigating the abrasive wear of the coating, in order to evaluate its suitability for applications where abrasion wear resistance is required, namely in the oil and gas industry, where the lifespan of pipelines could potentially be prolonged by this protective coating.

Previous work by the authors [19], investigating the scratch and indentation behavior, reported positive results for the Ni-P-Tribaloy composite coating regarding its properties in comparison with the Ni-P coating, especially its enhanced toughness. This work aims to fill the research gap regarding use of Tribaloy as reinforcement particles in electroless coatings, combining the advantages of the electroless plating method over other techniques and the high wear resistance of the alloy. The objective of this study is to assess the low-stress abrasion of the Ni-P-Tribaloy coating to further understand the coating's wear behavior. The ASTM G65 test is useful to determine the abrasion wear mechanisms. This present work will examine the wear scar, determine the operative wear mechanisms, and quantify the wear rate.

2. Materials and Methods

2.1. Coating Preparation

The substrates employed in this study were rectangular AISI 1018 steel specimens with dimensions of 25.4 mm by 76.2 mm and a thickness of 12.7 mm, in accordance with the size specified in the ASTM G65 standard. Table 1 shows the composition of AISI 1018. CoCrMoSi powder acquired from Nanoshel was employed as reinforcement particles in this composite coating. The composition of the powder was 29% molybdenum, 17% chromium, 3.5% silicon, and balance cobalt. The powder size distribution is shown in Figure 1. The powder analysis reveals a bimodal distribution. The major sizes found were 3 and 40 μm.

The values of the distribution D10, D50, and D90 were revealed as 1.65, 7.21, and 54.8 µm, respectively. The morphology of the as-received powder by scanning electron microscopy, or SEM, is shown in Figure 2.

Table 1. AISI 1018 steel chemical composition.

Element	C	Mn	Cu	Cr	Si	P	Fe
wt.%	0.182	0.754	0.186	0.181	0.095	0.04	Bal.

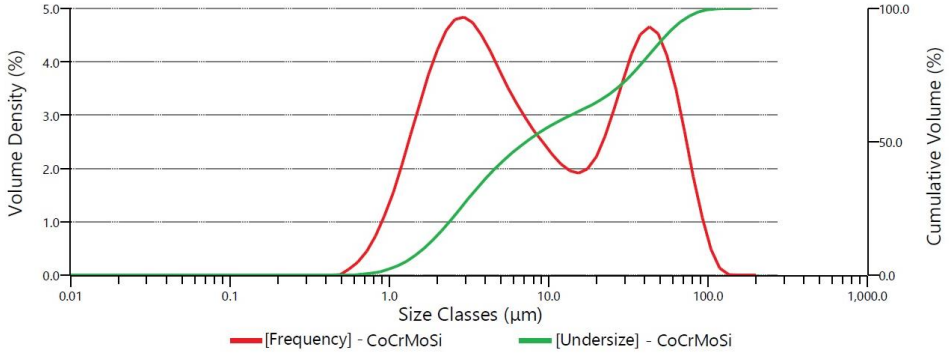

Figure 1. Tribaloy powder particle size distribution.

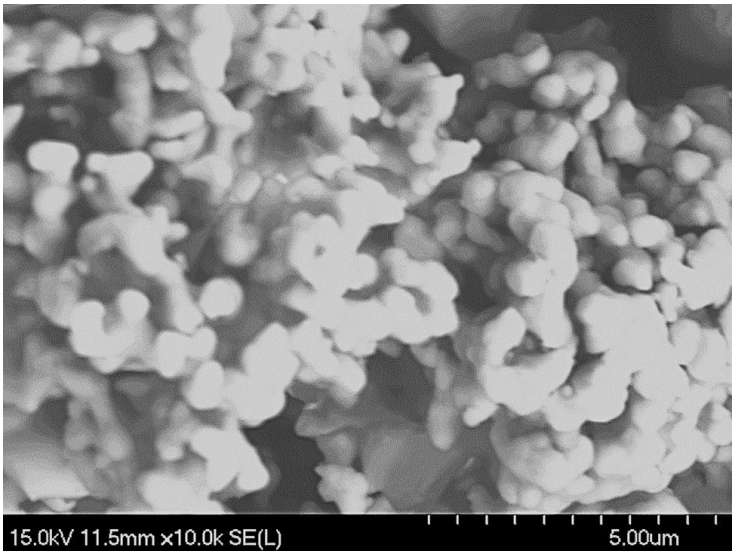

Figure 2. Tribaloy powder SEM image.

Prior to coating, the pre-treatment process consisted of grinding the steel specimens with 240, 320, 400, and 600 SiC abrasive papers, then polishing them with 9 µm diamond solution, followed by immersing in an alkali solution for 5 min at 80 ± 5 °C, and finally immersing in sulfuric acid (20 vol.%) for 15 s for surface activation. The alkali solution had the following ingredients: 30 g/L Na_3PO_4, 50 g/L NaOH, and 30 g/L Na_2CO_3. Rinsing of the specimens was carried out between every step with distilled water.

The prepared specimens were suspended inside a 1 L monolithic Ni-P plating bath for 40 min in order to deposit a thin pre-coating Ni-P layer for the purpose of improving the coating adhesion with the steel specimen. Then, the specimens were suspended in the composite 1 L plating bath containing Ni-P plating solution and 0.1 g/L powder concentration for 4.5 h at 88 ± 2 °C. Ammonium hydroxide was added as needed to maintain a pH of 4.7 ± 0.2. The plating duration of the monolithic Ni-P samples produced for comparison was 3 h.

2.2. Coating Characterization

The surface of the coating and its cross-section were inspected by confocal laser scanning microscopy (Keyence Corporation, Osaka, Japan), or CLSM, as well as scanning electron microscopy (Hitachi High-Tech, Tokyo, Japan). The composition of the coating was analyzed via energy dispersive spectroscopy employed by the SEM (EDS).

The microhardness values of the coatings were taken, in GPa, utilizing a PB 1000 mechanical tester from NANOVEA (NANOVEA Inc., Irvine, CA, USA). Microhardness tests were carried out on the polished surfaces of the coatings using a Vickers indenter with 6N of applied load. The repeatability of the recorded values was ensured by performing repeating the indents on both samples.

2.3. Low-Stress Abrasion Test

Low-stress abrasion tests were carried out according to ASTM G65 standards in order to evaluate the abrasion resistance using a dry sand/rubber wheel apparatus. The tests performed in this study followed procedure D as outlined in the ASTM G65 standard, which is a relatively lighter load variation of the test. This procedure is appropriate for thin coatings such as the coatings being tested here.

The force applied against the specimen in this test was 45 N, and the test was performed at 10-revolution increments, at 200 RPM, until coating failure was observed, which was indicated by the exposure of the substrate underneath the coating layer. The samples were weighed between each step (10 cycles) and recorded to express the abrasion rate in terms of material loss. A schematic diagram of the test apparatus is shown in Figure 3. A rubber wheel of 221.4 mm diameter and 12.84 mm width was used, along with semi-rounded silica sand having an average particle size of 212–300 µm. The particle size distribution is provided in Figure 4. The sand flow rate was between 300–400 g/min.

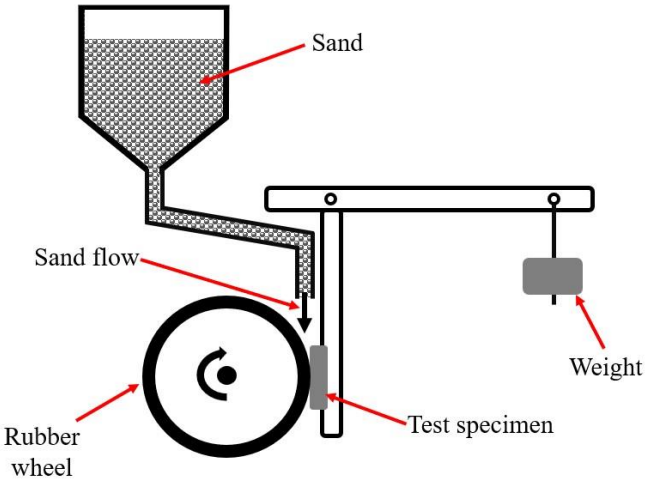

Figure 3. Schematic diagram of dry sand/rubber wheel test apparatus.

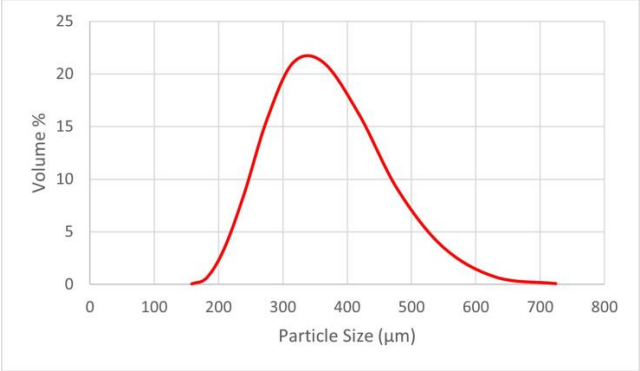

Figure 4. Silica sand particle size distribution.

3. Results

3.1. Coating Characterization

Composite Ni-P-Tribaloy coatings were successfully deposited on AISI 1018 steel substrates. A representative portion of the coating cross-section is shown in Figure 5, exhibiting excellent bonding at the substrate-coating interface and successful incorporation of the Tribaloy particles within the coating matrix. The thickness of the coating varies across the surface ranging from approximately 32 to 50 µm, including an 8 µm pre-coating layer for adhesion with the substrate. The variation in thickness is due to the presence of the Tribaloy particles in the coating as the larger particles themselves are being coated with Ni-P, as seen in Figure 5, resulting in thicker layers over large particles compared to areas with smaller particles. This occurrence has resulted in a rough surface of the composite Ni-P-Tribaloy coatings. The surface roughness value (Sa) was found to be 35 µm. SEM images of the surface and cross-section revealing the roughness of the coating surface is shown in Figure 6.

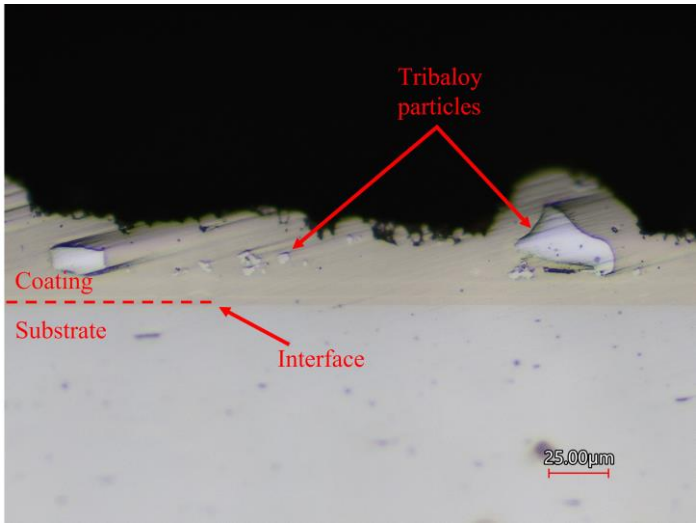

Figure 5. Cross-section of Ni-P-Tribaloy coating.

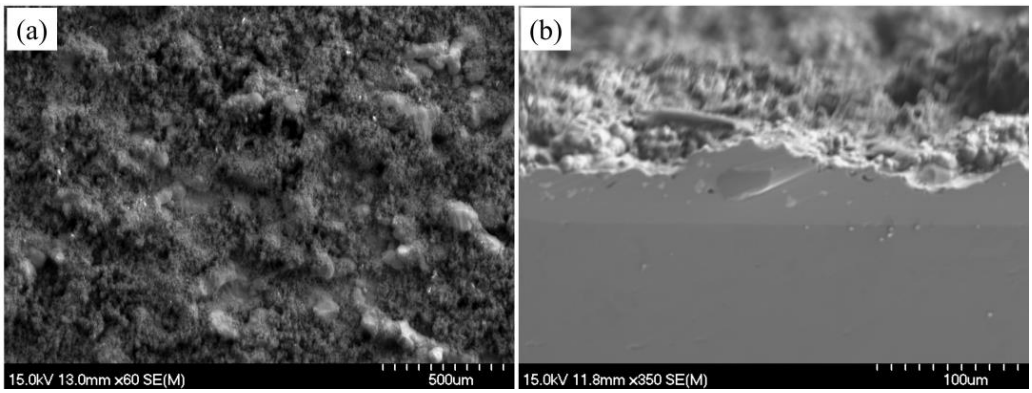

Figure 6. SEM image of Ni-P-Tribaloy coating (**a**) surface and (**b**) cross-section.

To determine the chemical composition of the coating, EDS analysis was carried out on its surface. Table 2 provides the Ni-P-Tribaloy composition by weight %. The existence of the four elements of the Tribaloy was confirmed in the coating: Co, Mo, Cr, and Si. Based on this composition, the coating is reported to consist of 16.5 wt.% of Tribaloy, or 15.7 vol.% Tribaloy, in the Ni-P matrix.

Table 2. Composition of Ni-P-Tribaloy.

Element	Ni	P	Cr	Mo	Si	Co
wt.%	74.62%	8.88%	3.94%	2.81%	1.42%	8.33%

The Vickers microhardness of the Ni-P-Tribaloy was determined as an average of four measurements and compared to monolithic Ni-P coating for comparison. Figure 7 graphically presents the average values for both types of coatings, with error bars that represent the measurements' standard deviation. The microhardness of the monolithic Ni-P coating is 5.36 GPa, falling within range of the microhardness in the literature: 5–6.5 GPa [26]. While the microhardness of the Ni-P-Tribaloy composite coating was found to be 6.00 GPa, which is 12% higher. The high hardness of the composite coating is ascribed to the presence of the much harder Tribaloy alloy particles in the Ni-P coating. Furthermore, AISI 1018 steel typically exhibits a microhardness of 1.7 GPa [22], significantly lower than that of both coatings.

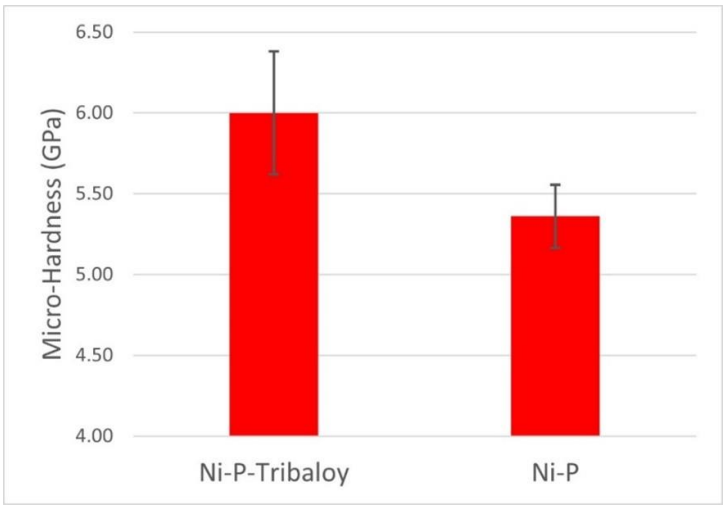

Figure 7. Microhardness values of Ni-P and Ni-P-Tribaloy.

3.2. Abrasion Wear Scar

Low-stress abrasion tests were performed on Ni-P-Tribaloy coating samples, as well as Ni-P coatings samples, until the steel substrates were first exposed and detected using visual inspection after each step. The resulting wear scars on both coatings are shown in Figure 8. The wear scars were rectangular in shape, fitting the description of an even and uniform scar as described in the ASTM G65 standard. This confirms the proper alignment of the apparatus setup and the accuracy of the test. The dimensions of the wear scars were roughly 25.4 mm long and 12.7 mm wide.

The 3D topographic scanning of the CLSM was utilized to analyze these wear scars. For each wear scar, a 3D scan was generated and the average profile across the scar width was produced by the averaging of 1500 horizontal lines at intervals of 5.3 μm across the middle, covering 7.95 mm of the middle of each scar, provided in Figure 9. It should be noted that the scar profile of the Ni-P coating is smoother as expected, because of the roughness of the Ni-P-Tribaloy coating surface prior to the abrasion leading to a rougher wear scar.

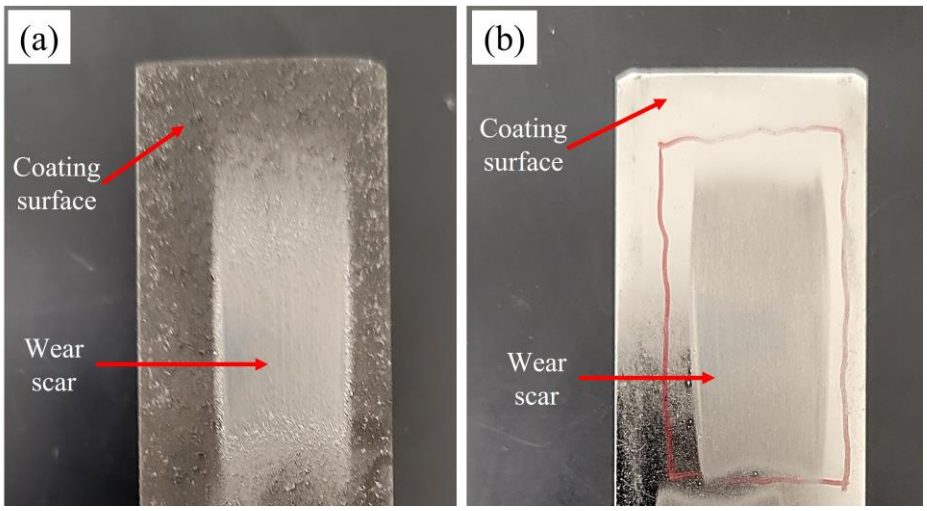

Figure 8. Pictures of wear scars on (**a**) Ni-P-Tribaloy and (**b**) Ni-P coating samples.

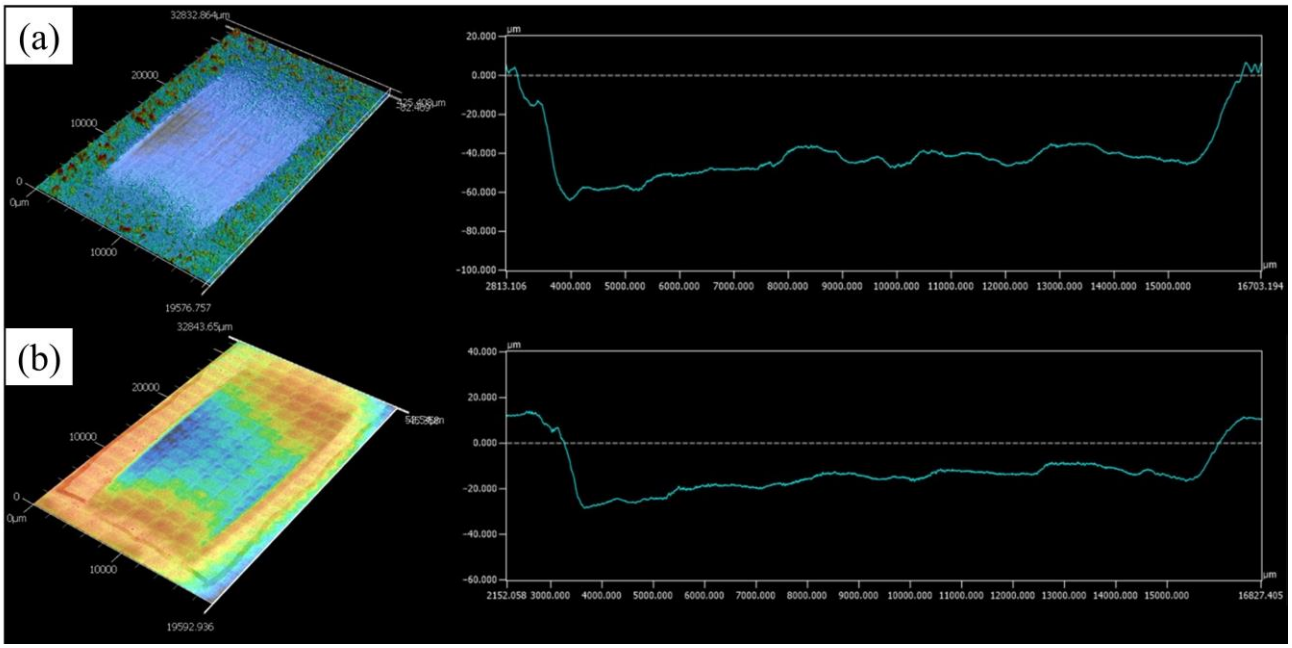

Figure 9. Shape and average profile of wear scars for (**a**) Ni-P-Tribaloy and (**b**) Ni-P.

3.3. Abrasion Rate

All specimens were weighed at the start of the abrasion test and continuously after each 10-revolution step to track the material loss due to abrasion. The tests results were expressed as volume loss in mm^3 in accordance with the ASTM G65 standard to allow for comparison with other materials. The cumulative abrasion volume loss is plotted in Figure 10 against the number of wheel revolutions for the Ni-P-Tribaloy and Ni-P coatings. The test was replicated on a separate sample for each material to ensure the repeatability of the results, and the average values were plotted with the standard deviation represented by error bars. The measurements for the Ni-P samples were extremely close in value; therefore, their error bars are too small to appear on the Ni-P curve.

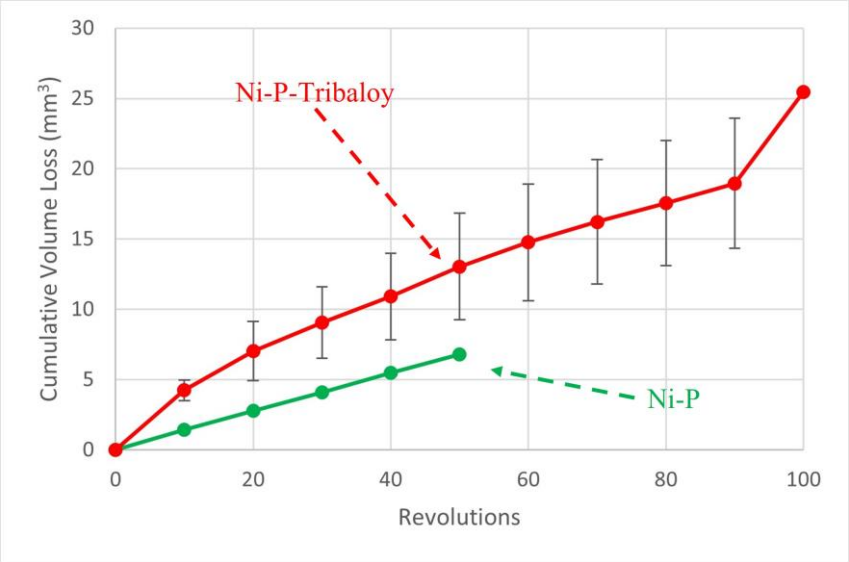

Figure 10. Abrasion volume loss against wheel revolutions.

One Ni-P-Tribaloy specimen was deemed to fail after 100 revolutions upon visual inspection and noticing the initial exposure of the steel. The second sample failed after 90 revolutions. On the other hand, both Ni-P specimens failed after only 50 revolutions. The number of revolutions is directly proportional to the degree of wear that the surface experiences. The volume loss for each case increases as wear is progressing, as expected, which follows the general model of abrasion [27]. It was revealed that the Ni-P-Tribaloy composite coating had experienced more volume loss compared to the monolithic Ni-P at any given point, under the exact same conditions. After 50 revolutions where the Ni-P coatings failed, the total volume loss of the Ni-P-Tribaloy and the Ni-P coatings were 13.0 and 6.80 mm^3, respectively. The high amount of volume loss in the Ni-P-Tribaloy coating is a result of the Tribaloy particles becoming detached as the surrounding Ni-P matrix is worn away, leaving holes in the coating surface, and subsequently, being caught under the rubber wheel and pushed against the test surface, adding to the three-body wear effect, that heavily influences the wear rate when the hard alloy particles are further sliding against the surface of the coating, wearing it out [28]. Studies have shown that the size of abrasive particles relative to the reinforcing particles in a metal matrix composite has an influence on wear, such that particle pull-out or plough-off becomes prominent during ASTM G65 testing when the abrasive particles are larger than the reinforcing particles, which is the case in this present study (Sections 2.1 and 2.3), as opposed to wear being primarily caused by the loss of matrix when the abrasive particles are small [29,30].

It is important to note that the Ni-P-Tribaloy coating specimens lasted longer in this test despite more material loss due to the discrepancy in the initial thicknesses. The Ni-P coatings tested in this study had a thickness of 33 μm, which is thinner than that of the composite coating discussed in Section 3.1. The Ni-P-Tribaloy wear scar was deeper and it was subject to more abrasion.

The abrasion wear rate was taken as the slope of the linear portion of the volume loss curve in mm^3 per revolution. It can be seen that the wear rate decreased with progressing wear for the Ni-P-Tribaloy coating, as the rough surface was flattened, while the wear rate of Ni-P remained constant throughout the experiment. The wear rate of the Ni-P-Tribaloy coating was calculated to be 0.170 mm^3 per revolution. In comparison, the Ni-P coating had a lower wear rate of 0.135 mm^3 per revolution. This can be attributed to the considerably higher roughness of the composite coating, as reported in several studies correlating higher wear rates to higher surface roughness [31–33].

3.4. Wear Scar Analysis

Upon the examination of the wear scar on the Ni-P-Tribaloy coating surface using SEM, the first feature observed at low magnification was the flattening of the coating surface. The rough coating surface prior to the test is due to some of the Tribaloy particles on the surface being coated over by the Ni-P around them, as discussed in Section 3.1, resulting in a high roughness by creating the asperities on the surface seen in Figures 5 and 6. The SEM images in Figure 11 illustrate the flattening that occurs at the edge of the abrasion wear scar, indicating their location on the scar. The insert images in the upper right corners are where the larger images were taken relative to the wear scar. It can be seen in Figure 11b that the surface at the edge of the wear scar is relatively smooth compared to the coating surface in Figure 6a using the same image scale, as the roughness is being flattened (rather than polished) due to the sliding. As the specimen was inspected further towards the middle of the scar, it was found that the surface is even smoother, as the asperities are being further flattened and pressed in. This is due to the nature of the contact between the rubber wheel and test specimen and their respective orientations as illustrated by the diagram in Figure 12 showing the contact area between the wheel and the specimen. There is less/shallower contact between the two at the edge of the wear scar and it undergoes less abrasion, whereas inside the scar there is deeper contact, thus more flattening of the material.

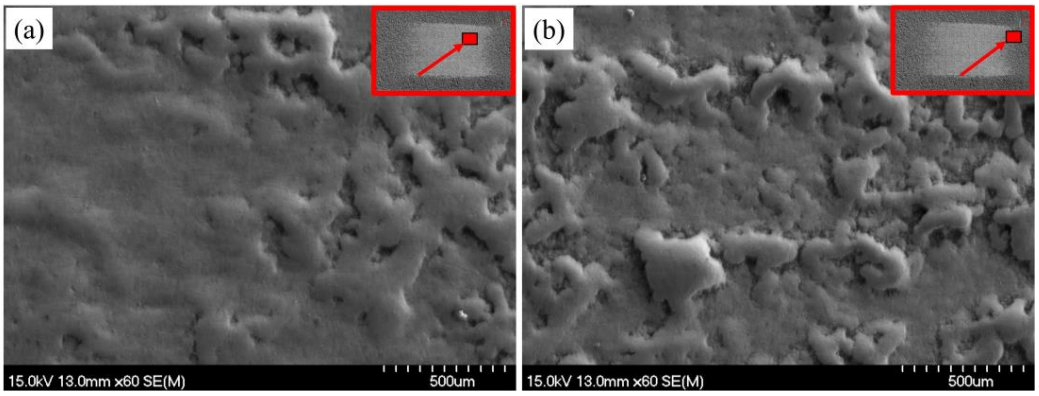

Figure 11. Abrasion surface depicting the flattening (**a**) inside and (**b**) at the edge of the scar.

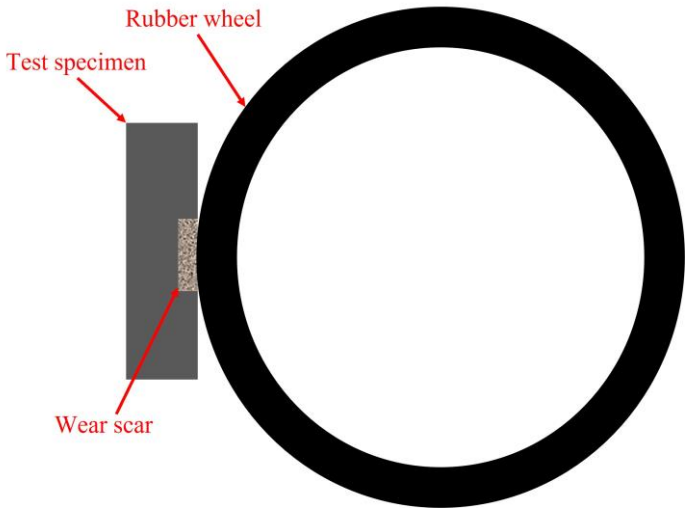

Figure 12. Illustrative diagram of the wheel–specimen contact area.

Figure 13 shows representative images of the abrasion from inside the wear scar. It was found that plowing is the dominant wear mechanism in the abrasion of this Ni-P-Tribaloy coating. Material is being is squeezed out and pushed to the sides to form ridges, which

is typical of the plowing mechanism. The coating is deformed by plastic deformation as each abrasive particle is extruding the surface and sliding over it. Large and semi-angular abrasive particles slide on the surface and cause wide and shallow grooves, as seen here, as opposed to deeper grooves and a cutting mechanism that would occur in the case of sharp abrasive particles with sharp corners, resulting in more damage. An instance of a deep groove, likely due to a sharp corner on an abrasive particle, is shown in Figure 14. Although some deep grooves that are indicative of a cutting mechanism were found, they were not significant, and they cannot be considered the dominant mechanism. It should be noted that the ridges formed do not slide in one direction; particles are being pushed against the surface and they slide in different directions, and the grooves intersect as seen in Figure 13a. The hardness of the Ni-P-Tribaloy coating also contributes to its wear resistance, as studies have shown that the penetration depth on the worn surface by the abrasive particles is proportional to the ratio of hardness to applied force [34,35].

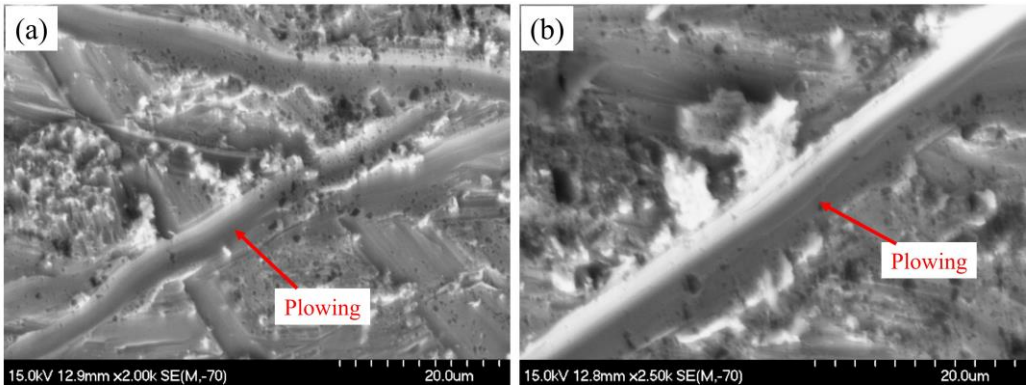

Figure 13. SEM images of grooves formed by plowing on Ni-P-Tribaloy at (**a**) lower and (**b**) higher magnification.

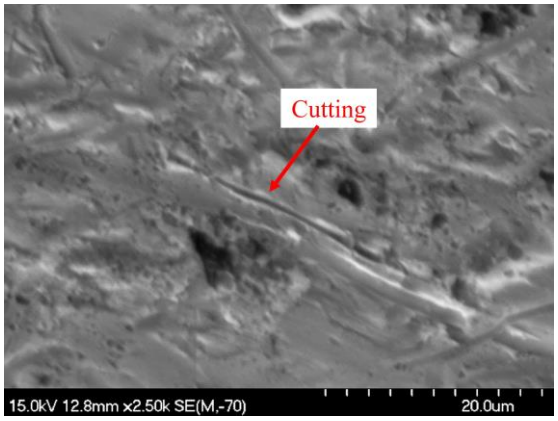

Figure 14. An example of a cutting deep groove on Ni-P-Tribaloy.

Furthermore, there is also compaction that occurs, along with plowing, arising from the applied load and the contact between the rough surface and the rubber, where the material is pressed in by that contact. Areas where the rough surface is being pressed in can be seen in the SEM image provided in Figure 15, while in the Ni-P samples in Figure 16, mainly plowing is present. The compaction in the Ni-P-Tribaloy abrasion can be attributed to the hardness of the Tribaloy particles. They cannot be easily removed from the coating by plowing, the coating is plowed over them and they are compressed in. This is also evident in Figure 17, showing the cross-section, where the Tribaloy particles are protruding from the Ni-P matrix while the material around them is removed by plowing, and subsequently the particles are removed.

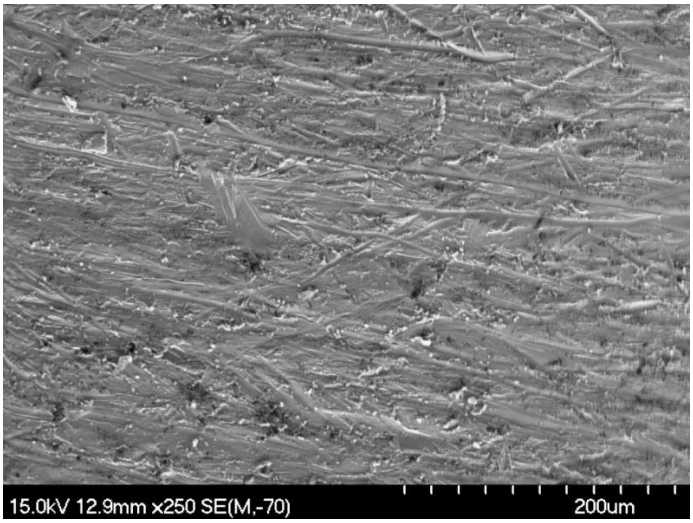

Figure 15. SEM image of Ni-P-Tribaloy abrasion wear scar.

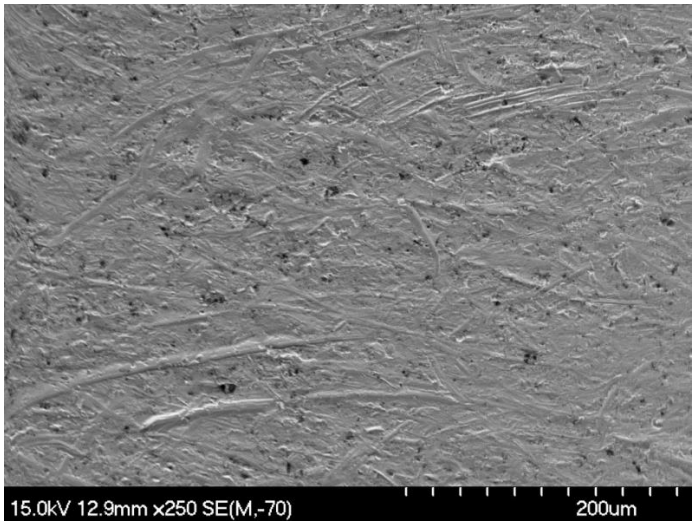

Figure 16. SEM image of Ni-P abrasion wear scar.

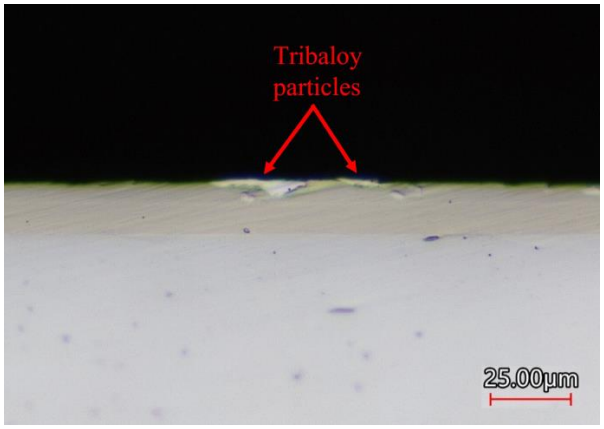

Figure 17. Cross-section of wear scar showing protruding particles.

4. Discussion

Based on the findings presented in this work, the wear mechanism of the Ni-P-Tribaloy composite coating can be described as follows: the Ni-P matrix above and around the

Tribaloy particles is plastically deformed by the plowing mechanism while the particles are held in the matrix. Once the matrix around the particles is worn out and the particles are protruding, the particles are then pulled out, leaving large gaps as they are large particles. The continuous plowing carries on removing the matrix material until the entire coating thickness is worn out. This mechanism is illustrated in the schematic given in Figure 18. The four steps are plowing of the matrix, protrusion of reinforcement particles, particle pull-out, and removal of the rest of the matrix while the trapped reinforcement particles contribute to the three-body abrasive wear. A similar wear mechanism was reported by Surzhenkov et al. [36], who observed the wear process happening in two stages in which the matrix was first destroyed and then the loose reinforcement particles (WC-Co) were lost.

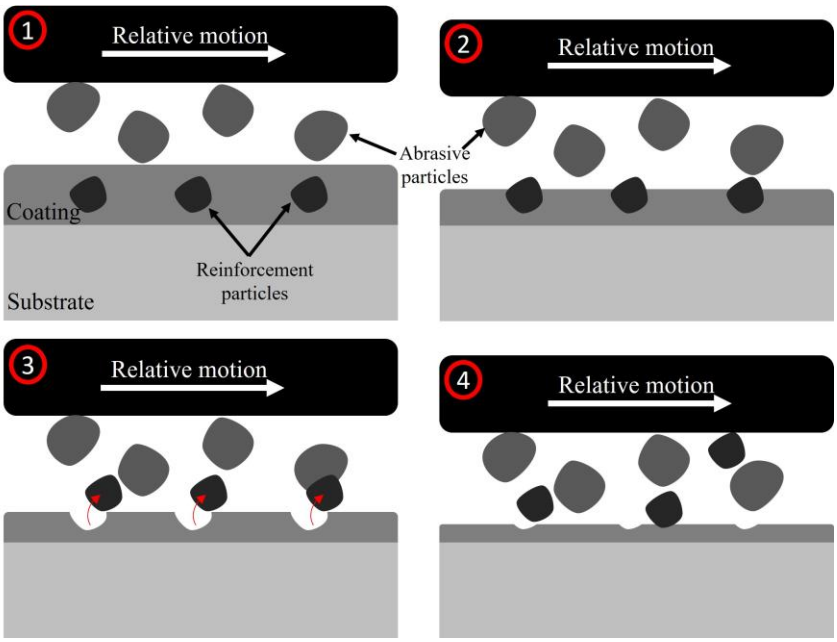

Figure 18. Schematic diagram of MMC wear mechanism during dry sand/rubber wheel abrasion.

Instances of this mechanism were captured with SEM in the abraded cross-section of the composite, verifying the existence of this wear mechanism. Figure 19a points out a Tribaloy particle, in the worn-out matrix, that is slightly protruding and on the verge of being exposed as the Ni-P matrix around it continues to undergo further wear. This particle would then protrude out of the matrix enough to be pulled out of the matrix. Figure 19b reveals areas of particle removal where the pulled out Tribaloy particles leave gaps in the matrix where they were once situated. It should be noted that these images are from different locations in the coating; however, they depict the steps outlined here as they are in different stages of the wear mechanism and they would follow the same steps under further wear.

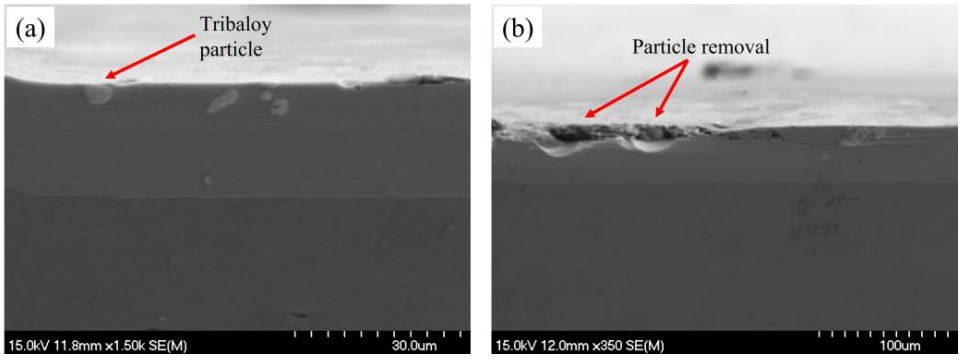

Figure 19. SEM images (**a**) before and (**b**) after Tribaloy particle removal.

Regarding the particle removal process itself within the described wear mechanism, consider the microscopic image given in Figure 20. It can be seen that the Tribaloy particle is beginning to detach from the matrix, likely accelerated by delamination. Delamination occurs under loading where the cracks develop beneath the surface at maximum shear stress and extend parallel to the surface, ultimately causing delamination. When reinforcement particles are present, delamination will occur at the interface between the matrix and the particle as it is a weaker area compared to the matrix and the particles. Researchers have reported that the interface plays an important role in this delamination mechanism. The particle-matrix interface has been established in the literature as a favorable area for crack formation and propagation during sliding wear of metal matrix composites (MMC), and that interfacial bond is stronger when the reinforcement particles are nano-sized over micro-sized [37–39]. Thus, the Tribaloy particle in Figure 20 is exhibiting detachment caused by delamination at the coating particle–matrix interface.

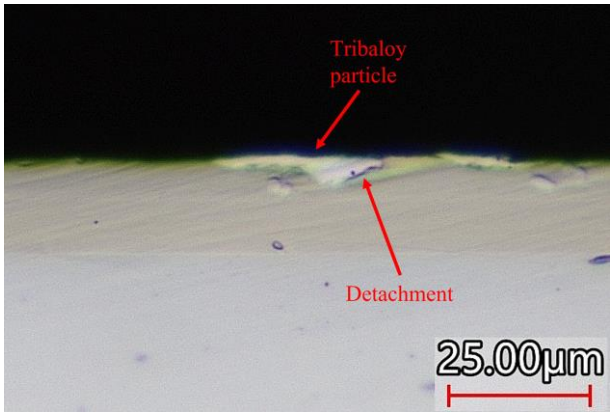

Figure 20. Tribaloy particle detachment from Ni-P matrix.

Hence, the controlling parameters influencing the wear mechanism of the Ni-P-Tribaloy coating are the sizes of the reinforcing particles and abrasive particles, and the hardness of the overall coating matrix, the reinforcing particles, and abrasive particles.

Reddy et al. [40] suggested that the integrity of a Ni-P composite coatings can be improved with smaller particles, as they are easier to be held by the matrix in a study that ascribed worse wear resistance to larger second-phase particles. The higher wear rate of the Ni-P-Tribaloy compared to the monolithic Ni-P coating in the results (Section 3.3) was mainly attributed to the high surface roughness and particle pull-out; both are directly linked to the large Tribaloy particle size. Moreover, studies comparing micro- and nano-sized particles in MMCs have shown that micro-sized particles exhibit higher wear loss due to delamination, while nano-sized particles provided better resistance to delamination due to having stronger bonding at the particle-matrix interface where delamination occurs [37,39]. Additionally, larger particles leave larger gaps when they are pulled out; hence, the measured wear loss will be higher.

Particle pull-out was also linked to the abrasive particles size in the results presented earlier. The larger the abrasive particles, the more prominent particle pull-out becomes over wear by loss of matrix. Additionally, the more rounded the abrasive particles are, the more dominant plowing becomes over cutting, which is more severe and leads to deeper grooves when the abrasives have sharp edges [41]. Some micro-cutting was observed here, because the abrasive particles used are semi-angular. The literature suggests that micro-cutting is present when the hardness of the abrasives are higher than the hardness of the abraded surface [36]. The composite coating hardness is 6.00 GPa, and the Ottawa silica sand used in this test typically has hardness values of around 10.7–13.0 GPa [42,43].

The overall hardness of the composite coating matrix influences the wear resistance positively such that depth of the wear grooves on the abraded surface is shallower when the surface of the material is harder. The hardness of the Tribaloy particles themselves

makes it more difficult for them to be pulled out from the matrix from plowing. Wear loss from particle pull-out is discussed extensively in this study; however, as long as the particles are embedded in the matrix and not protruding out of it, they are able to resist plowing. The hardness of the Tribaloy particles is also evident in all the provided figures where none of particles were fractured at different stages of wear.

5. Conclusions

Electroless Ni-P-Tribaloy composite coatings were prepared on AISI 1018 steel and tested under low-stress abrasion according to ASTM G65 standards to investigate their abrasion wear thoroughly. The composite coating had a composition of 15.7 vol.% Tribaloy and a thickness of 32–50 μm, with high surface roughness associated with this variation in thickness. The microhardness was measured to be 6.00 GPa with a Vickers indenter.

Uniform and even wear scars were observed on the test surfaces after the abrasion tests were carried out. The Ni-P-Tribaloy tests lasted 90 and 100 revolutions before failure, defined as the first appearance of the steel substrate, while the thinner Ni-P coating samples lasted 50 revolutions. The volume loss after 50 revolutions were 13.0 and 6.80 mm^3 for Ni-P-Tribaloy and the Ni-P, respectively. Additionally, the wear rates were calculated to be 0.170 and 0.135 mm^3 per revolution, respectively. The composite experienced higher loss of volume because of the large size of Tribaloy particles being pulled out of the track and amplifying the three-body wear.

Flattening of the roughness was noted by examining the edge of the wear scar and comparing areas inside and outside of the scar. The plowing mechanism was determined to be the dominant wear mechanism in the low-stress abrasion of the Ni-P-Tribaloy coating. The coating surface was plastically deformed as the material was extruded to the sides by the round abrasive particles sliding over it, creating wide and shallow grooves. Compaction was also observed in the wear scar as the coating matrix was pressed over the Tribaloy particles, indicative of the high hardness of the particles.

The wear mechanism of the composite Ni-P-Tribaloy coating has two main stages: plowing of the Ni-P matrix, followed by the removal of the Tribaloy particles. The particle removal process is caused by delamination that occurs at the coating particle–matrix interface. The controlling parameters of the wear mechanism are the sizes of the reinforcing particles and abrasive particles, and the hardness values of the overall coating matrix, the reinforcing particles, and abrasive particles. The large size of the Tribaloy contributes significantly to the wear of the composite coating as it increases the roughness, leaves large gaps, and enhances the delamination at the particle–matrix interface bonding. Further studies are needed using finer (nano-sized) Tribaloy particles in an effort to improve the wear resistance of the composite coating.

Author Contributions: Conceptualization, Z.F.; methodology, A.M., Z.F. and M.A.I.; formal analysis, A.M.; investigation, A.M.; resources, Z.F.; data curation, M.A.I.; writing—original draft preparation, A.M.; writing—review and editing, Z.F.; supervision, Z.F. All authors have read and agreed to the published version of the manuscript.

Funding: This research was funded by the Natural Sciences and Engineering Research Council of Canada (NSERC), grant number RGPIN 05125-17.

Institutional Review Board Statement: Not applicable.

Informed Consent Statement: Not applicable.

Data Availability Statement: The data presented in this study are available on request from the corresponding author.

Conflicts of Interest: The authors declare no conflict of interest.

References

1. Slota, J.; Kubit, A.; Gajdoš, I.; Trzepieciński, T.; Kaščák, Ľ. A Comparative Study of Hardfacing Deposits Using a Modified Tribological Testing Strategy. *Lubricants* **2022**, *10*, 187. [CrossRef]

2. Franco, M.; Sha, W.; Malinov, S.; Liu, H. Micro-Scale Wear Characteristics of Electroless Ni–P/SiC Composite Coating under Two Different Sliding Conditions. *Wear* **2014**, *317*, 254–264. [CrossRef]
3. Fayyad, E.M.; Abdullah, A.M.; Hassan, M.K.; Mohamed, A.M.; Jarjoura, G.; Farhat, Z. Recent Advances in Electroless-Plated Ni-P and Its Composites for Erosion and Corrosion Applications: A Review. *Emergent Mater.* **2018**, *1*, 3–24. [CrossRef]
4. Balaraju, J.N.; Priyadarshi, A.; Kumar, V.; Manikandanath, N.T.; Kumar, P.P.; Ravisankar, B. Hardness and Wear Behaviour of Electroless Ni–B Coatings. *Mater. Sci. Technol.* **2016**, *32*, 1654–1665. [CrossRef]
5. Loto, C.A. Electroless Nickel Plating—A Review. *Silicon* **2016**, *8*, 177–186. [CrossRef]
6. Brenner, A.; Riddell, G.E. Nickel Plating on Steel by Chemical Reduction. *J. Res. Natl. Bur. Stan.* **1946**, *37*, 31. [CrossRef]
7. Mallory, G.O.; American Electroplaters and Surface Finishers Society (Eds.) *Electroless Plating: Fundamentals and Applications*; American Electroplaters and Surface Finishers Soc: Orlando, FL, USA, 1990.
8. Luo, H.; Leitch, M.; Behnamian, Y.; Ma, Y.; Zeng, H.; Luo, J.-L. Development of Electroless Ni–P/Nano-WC Composite Coatings and Investigation on Its Properties. *Surf. Coat. Technol.* **2015**, *277*, 99–106. [CrossRef]
9. De Hazan, Y.; Zimmermann, D.; Z'graggen, M.; Roos, S.; Aneziris, C.; Bollier, H.; Fehr, P.; Graule, T. Homogeneous Electroless Ni–P/SiO2 Nanocomposite Coatings with Improved Wear Resistance and Modified Wear Behavior. *Surf. Coat. Technol.* **2010**, *204*, 3464–3470. [CrossRef]
10. Li, Z.; Farhat, Z.; Jarjoura, G.; Fayyad, E.; Abdullah, A.; Hassan, M. Synthesis and Characterization of Scratch-Resistant Ni-P-Ti-Based Composite Coating. *Tribol. Trans.* **2019**, *62*, 880–896. [CrossRef]
11. Agarwala, R.C.; Agarwala, V. Electroless Alloy/Composite Coatings: A Review. *Sadhana* **2003**, *28*, 475–493. [CrossRef]
12. Huang, Y.S.; Zeng, X.T.; Annergren, I.; Liu, F.M. Development of Electroless NiP–PTFE–SiC Composite Coating. *Surf. Coat. Technol.* **2003**, *167*, 207–211. [CrossRef]
13. Alidokht, S.A.; Gao, Y.; de Castilho, B.C.N.M.; Sharifi, N.; Harfouche, M.; Stoyanov, P.; Makowiec, M.; Moreau, C.; Chromik, R.R. Microstructure and Mechanical Properties of Tribaloy Coatings Deposited by High-Velocity Oxygen Fuel. *J. Mater. Sci.* **2022**, *57*, 20056–20068. [CrossRef]
14. Xu, W.; Liu, R.; Patnaik, P.C.; Yao, M.X.; Wu, X.J. Mechanical and Tribological Properties of Newly Developed Tribaloy Alloys. *Mater. Sci. Eng. A* **2007**, *452–453*, 427–436. [CrossRef]
15. Nsoesie, S.; Liu, R.; Jiang, K.; Liang, M. High-Temperature Hardness and Wear Resistance of Cobalt-Based Tribaloy Alloys. *Int. J. Mech. Mater. Eng.* **2013**, *2*, 48–56.
16. Cameron, C.B.; Ferriss, D.P. Tribaloy Intermetallic Materials: New Wear- and Corrosion-Resistant Alloys. *Anti-Corros. Meth Mater.* **1975**, *22*, 5–8. [CrossRef]
17. Liu, R.; Yao, J.; Zhang, Q.; Yao, M.X.; Collier, R. Effects of Silicon Content on the Microstructure and Mechanical Properties of Cobalt-Based Tribaloy Alloys. *J. Eng. Mater. Technol.* **2016**, *138*, 041017. [CrossRef]
18. Durejko, T.; Łazińska, M.; Dworecka-Wójcik, J.; Lipiński, S.; Varin, R.A.; Czujko, T. The Tribaloy T-800 Coatings Deposited by Laser Engineered Net Shaping (LENSTM). *Materials* **2019**, *12*, 1366. [CrossRef]
19. Mabrouk, A.; Farhat, Z. Novel Ni-P-Tribaloy Composite Protective Coating. *Materials* **2023**, *16*, 3949. [CrossRef]
20. Bhushan, B. *Principles and Applications of Tribology*, 2nd ed.; Tribology series; Wiley: Chichester, UK, 2013.
21. Hutchings, I.; Shipway, P. *TRIBOLOGY: Friction and Wear of Engineering Materials*, 2nd ed.; Elsevier: Cambridge, MA, USA, 2017.
22. Li, Z. *Electroless Ni-P-Ti Based Nanocomposite Coatings*; Dalhousie University: Halifax, NS, USA, 2021.
23. Hyttel, M.W.; Olsson, D.D.; Reisel, G.; Bøttiger, J. Comparison of a Newly Developed Compression-Twist Abrasive Wear Test with the ASTM G65 Test Method. *Wear* **2013**, *307*, 134–141. [CrossRef]
24. *G65-16*; Standard Test Method for Measuring Abrasion Using the Dry Sand/Rubber Wheel Apparatus. ASTM International: West Conshohocken, PA, USA, 2017.
25. Hawk, J.A.; Wilson, R.D.; Tylczak, J.H.; Doğan, Ö.N. Laboratory Abrasive Wear Tests: Investigation of Test Methods and Alloy Correlation. *Wear* **1999**, *225–229*, 1031–1042. [CrossRef]
26. Jensen, R.; Farhat, Z.; Islam, M.A.; Jarjoura, G. Effect of Coating Thickness on Wear Behaviour of Monolithic Ni-P and Ni-P-NiTi Composite Coatings. *Solids* **2022**, *3*, 620–642. [CrossRef]
27. Kamdi, Z.; Shipway, P.H.; Voisey, K.T.; Sturgeon, A.J. Abrasive Wear Behaviour of Conventional and Large-Particle Tungsten Carbide-Based Cermet Coatings as a Function of Abrasive Size and Type. *Wear* **2011**, *271*, 1264–1272. [CrossRef]
28. Kašparová, M.; Zahálka, F.; Houdková, Š. WC-Co and Cr3C2-NiCr Coatings in Low- and High-Stress Abrasive Conditions. *J. Therm. Spray Technol.* **2011**, *20*, 412–424. [CrossRef]
29. Liyanage, T.; Fisher, G.; Gerlich, A.P. Microstructures and Abrasive Wear Performance of PTAW Deposited Ni–WC Overlays Using Different Ni-Alloy Chemistries. *Wear* **2012**, *274–275*, 345–354. [CrossRef]
30. Hu, J.; Li, D.Y.; Llewellyn, R. Synergistic Effects of Microstructure and Abrasion Condition on Abrasive Wear of Composites—A Modeling Study. *Wear* **2007**, *263*, 218–227. [CrossRef]
31. Al-Samarai, R.A.; Haftirman; Ahmad, K.R.; Al-Douri, Y. Evaluate the Effects of Various Surface Roughness on the Tribological Characteristics under Dry and Lubricated Conditions for Al-Si Alloy. *J. Surf. Eng. Mater. Adv. Technol.* **2012**, *2*, 167–173. [CrossRef]
32. Hisakado, T. The Influence of Surface Roughness on Abrasive Wear. *Wear* **1977**, *41*, 179–190. [CrossRef]
33. Hadinezhad, M.; Elyasi, M.; Rajabi, M.; Abbasi, M. Study of the Effects of Slip Distance and Surface Roughness on Wear Rate. *MST* **2015**, *3*, 146–154. [CrossRef]

34. Panziera, R.C.; Flores, W.H.; Tier, M.A.D.; De Oliveira, A.C.C. Comparison of Abrasive Wear by Rice Husk of an HVOF WC–Co–Cr-Based Coating and an Electric Arc Sprayed Coating Based on Fe–Cr–B–Si. *J. Braz. Soc. Mech. Sci. Eng.* **2019**, *41*, 331. [CrossRef]
35. Rabinowicz, E.; Dunn, L.A.; Russell, P.G. A Study of Abrasive Wear under Three-Body Conditions. *Wear* **1961**, *4*, 345–355. [CrossRef]
36. Surzhenkov, A.; Viljus, M.; Simson, T.; Tarbe, R.; Saarna, M.; Casesnoves, F. Wear Resistance and Mechanisms of Composite Hardfacings at Abrasive Impact Erosion Wear. *J. Phys. Conf. Ser.* **2017**, *843*, 012060. [CrossRef]
37. Moazami-Goudarzi, M.; Akhlaghi, F. Wear Behavior of Al 5252 Alloy Reinforced with Micrometric and Nanometric SiC Particles. *Tribol. Int.* **2016**, *102*, 28–37. [CrossRef]
38. Sannino, A.P.; Rack, H.J. Dry Sliding Wear of Discontinuously Reinforced Aluminum Composites: Review and Discussion. *Wear* **1995**, *189*, 1–19. [CrossRef]
39. Kang, Y.-C.; Chan, S.L.-I. Tensile Properties of Nanometric Al2O3 Particulate-Reinforced Aluminum Matrix Composites. *Mater. Chem. Phys.* **2004**, *85*, 438–443. [CrossRef]
40. Reddy, V.V.N.; Ramamoorthy, B.; Nair, P.K. A Study on the Wear Resistance of Electroless Ni–P/Diamond Composite Coatings. *Wear* **2000**, *239*, 111–116. [CrossRef]
41. Stachowiak, G.W.; Batchelor, A.W. *Engineering Tribology*, 4th ed.; Elsevier Butterworth-Heinemann: Amsterdam, The Netherlands; Heidelberg, Germany, 2014.
42. Erdoğan, S.T.; Forster, A.M.; Stutzman, P.E.; Garboczi, E.J. Particle-Based Characterization of Ottawa Sand: Shape, Size, Mineralogy, and Elastic Moduli. *Cem. Concr. Compos.* **2017**, *83*, 36–44. [CrossRef]
43. Daphalapurkar, N.P.; Wang, F.; Fu, B.; Lu, H.; Komanduri, R. Determination of Mechanical Properties of Sand Grains by Nanoindentation. *Exp. Mech.* **2011**, *51*, 719–728. [CrossRef]